IEEE Access
Multidisciplinary | Rapid Review | Open Access Journal

Received January 29, 2019, accepted March 1, 2019, date of publication March 13, 2019, date of current version May 22, 2019.

Digital Object Identifier 10.1109/ACCESS.2019.2904524

A New High-Performance LED Converter With Separation of the AC and DC Driving Parts for a T8 LED Tube

SUNG HWAN KIM, (Member, IEEE), AND SEOK-HYUN LEE, (Member, IEEE)
Electrical Engineering Department, Inha University, Incheon 22212, South Korea

Corresponding author: Seok-Hyun Lee (plasma@inha.ac.kr)

This work was supported in part by the Inha University Research Grant 59181-1.

ABSTRACT This paper proposes a new high-performance light-emitting diode (LED) converter with separation of the AC and DC driving parts for a T8 LED tube. The proposed LED converter is mounted at the end of the LED tube in G13 base and G13 base dummy. The separation of the AC and DC driving parts enhances the light uniformity of the LED tube by securing the optical distance between the optic cover and light source. The AC driving part was designed to be inserted in a G13 base and was connected with the DC driving part through an LED module. The proposed LED converter is based on single-stage buck-boost topology and was designed for the operation at 19 W for a 1200 mm T8 LED tube. The proposed LED converter is very small and has fewer parts than other LED converters but still has high performance. The measurement results of the proposed LED converter show that the line regulation of the LED output current is less than 3.4% at 100-240 VAC and achieves high circuit efficiency (>89%), high power factor (>0.93), and low total harmonic distortion (<9%). In addition, all the current harmonics of the converter meet the requirements of the IEC 61000-3-2 Class C standards for high-performance LED lighting applications.

INDEX TERMS LED converter, single-stage buck-boost, T8 LED tube, AC and DC separation, high circuit efficiency, high power factor, low total harmonic-distortion, current harmonics.

I. INTRODUCTION

Light-emitting diodes (LEDS) have been widely used in lighting applications due to the advantages of high luminous efficacy, low power consumption, long lifetime, and eco-friendliness. Many LED retrofit lamps have been developed, such as LED candles, LED bulbs, and LED tubes. These are gradually replacing conventional lighting, such as incandescent lamps and fluorescent lamps [1], [2]. LED tubes are a type of LED retrofit lamp with various lamp bases and are used to replace traditional fluorescent tubes. There are many kinds of LED tubes, which have different lamp lengths, lamp diameters, and bases.

Fig. 1(b) shows a longitudinal view of a conventional T8 LED tube, which is composed of various parts. For installation on a luminaire, there is a G13 base and a G13 dummy on both sides of the LED tube, which has a semi-circular metal heatsink inside it with an LED module. It is assembled with an optic cover and contains an LED converter. Generally, the heatsink of the LED tube plays three roles: removing heat from the LED module, preventing the LED tube from bending, and enclosing the LED converter.

However, there are some problems in a conventional LED tube. First, as the length of the LED tube increases, the weight of the product increases sharply because of the heatsink. Second, the space inside the heatsink is very small, so the selection of parts of the LED converter on a printed circuit board (PCB) is limited. The LED converter must also be insulated from the heatsink. Above all, it is difficult to obtain enough optical distance for uniform light diffusion due to the height of the LED converter, which makes a hot spot on the optic cover and decreases the light uniformity. As shown in Fig. 1(a), there is trade-off relation between the optical distance and the height of the LED converter. To achieve good uniformity without a hot spot, an optic cover with higher haze needs to be applied, or more LEDs need to be mounted on the PCB, which increases the total cost [3]–[6].

The associate editor coordinating the review of this manuscript and approving it for publication was Tariq Masood.

2169-3536 © 2019 IEEE. Translations and content mining are permitted for academic research only.
Personal use is also permitted, but republication/redistribution requires IEEE permission.
See http://www.ieee.org/publications_standards/publications/rights/index.html for more information.

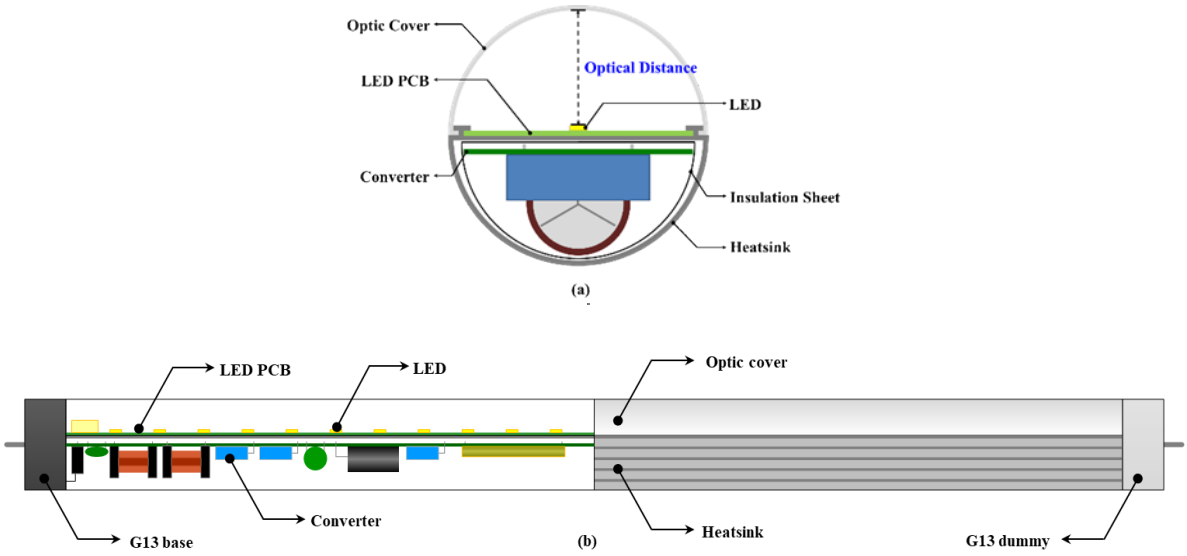

FIGURE 1. (a) Cross-sectional view of a conventional T8 LED tube, (b) Longitudinal sectional view.

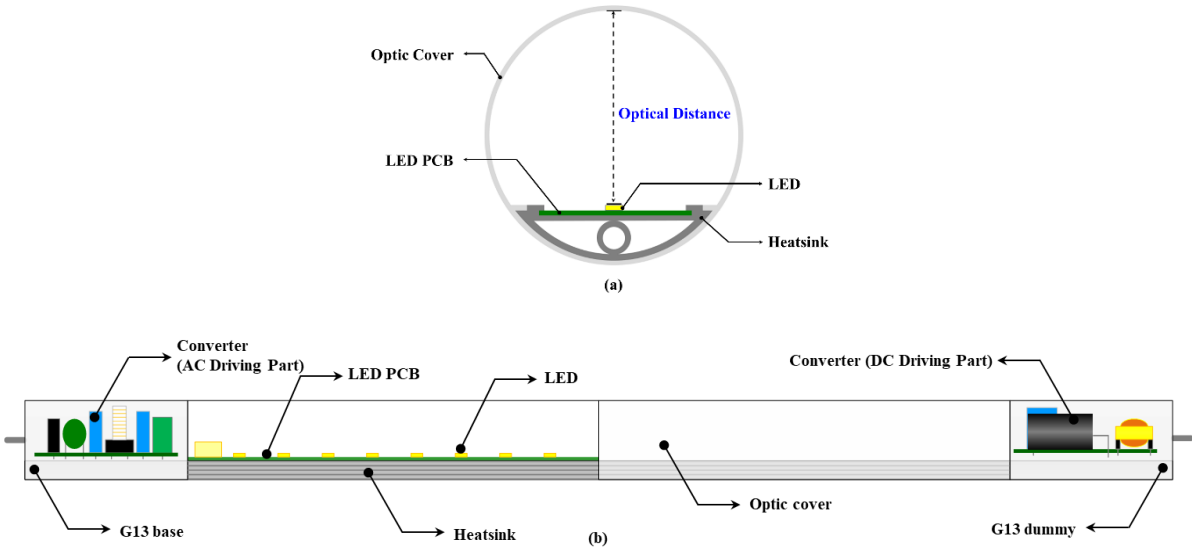

FIGURE 2. (a) Cross-sectional view of a T8 LED tube with the proposed LED converter, (b) Longitudinal sectional view.

To overcome these problems while maintaining high performance, this paper proposes a new single-stage buck-boost LED converter with separation of the AC and DC driving parts for a T8 LED tube. It features small size and fits in a G13 base and G13 dummy, which has a 28 mm diameter, high efficiency, and high PF. In section II, the mechanical design of the proposed LED converter is described in detail, and in Section III, the electrical design is explained. In Section IV, the experimental results are discussed, and finally, the conclusions are given in Section V.

II. MECHANICAL DESIGN

A. AC AND DC DRIVING PART SEPARATION

Fig. 2(b) shows the longitudinal sectional view of a T8 LED tube with the proposed LED converter. It consists of a metal heatsink with an LED module inside and an optical enclosure. The AC and DC driving parts are inserted in the G13 base and G13 base dummy, respectively. The proposed LED converter is located at both sides of the LED tube.

By using the AC and DC driving parts separation, as shown in Fig. 2(a), the heatsink size is minimized to obtain a higher optical distance without having a critical influence on the heat radiation of the LED module. Although the two driving parts are disconnected, they are electrically connected to each other through the LED module. As shown in Fig. 3, VDC is rectified by a bridge rectifier from the input AC line in the

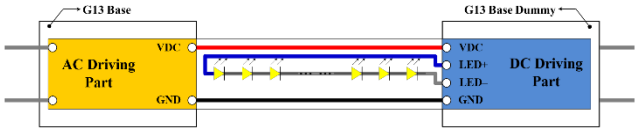

FIGURE 3. Internal connection diagram of T8 LED tube with the proposed LED converter.

AC driving part and is transferred to the DC link capacitor in the DC driving part through the copper patterns on the LED PCB. The DC driving part generates a constant current that is supplied to the LED arrays.

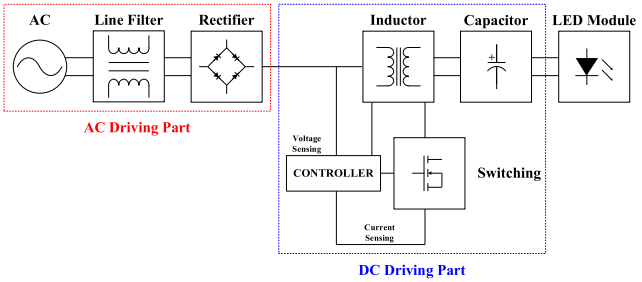

FIGURE 4. Block diagram of the proposed LED converter.

B. MOUNT STRUCTURE INSIDE OF THE G13 ENCLOSURE

Fig. 4 presents a block diagram of the proposed LED converter, which is composed of many function blocks. With consideration for the circuit function and size, the proposed LED converter is divided into AC and DC driving parts. The AC driving part consists of the AC input, a line filter block made of some capacitors and coils for noise suppression, a rectifier block, and some safety components. The DC driving part is composed of an inductor, a switching block with gate control circuitry, and a capacitor block for smoothing the LED output voltage.

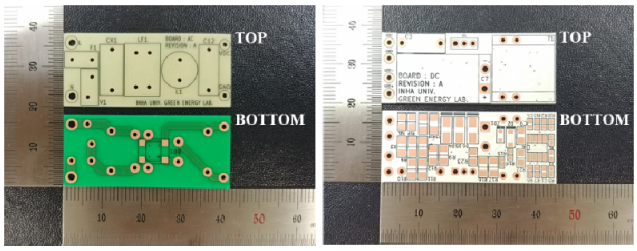

FIGURE 5. PCB outline of (a) the AC driving part, (b) the DC driving part.

Fig. 5 shows the PCB outlines of the AC and DC driving parts. The PCB for the AC driving part is made of a single-sided CEM-3 with 1T thickness and an area of 18 mm × 42 mm (W×L). For the DC driving part, the PCB is made of double-sided FR-4 with 1T thickness and an area of 18 mm × 45 mm (W×L). Fig. 6 shows a side view of the assembled prototype. In the AC driving part, all of the components mounted on the top side are manually inserted parts except the bridge rectifier on the bottom side of the PCB. However, most of the components in the DC driving part are surface-mount devices (SMDs) on the bottom side of the PCB except the inductor, MOSFET, and some capacitors. Each driving part is enclosed by the G13 base and G13 base dummy for insulation and must be designed to fit inside an LED tube with diameter limited to 28 mm or less according

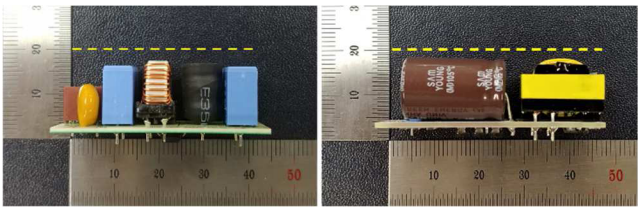

FIGURE 6. Side view of (a) the AC driving part prototype, (b) the DC driving part prototype.

to the IEC standards [7]. As shown in Fig. 6, the maximum height is not more than 20 mm.

TABLE 1. Outline information of the main components.

Component		Width × Length (mm)	Height (mm)
AC Driving Part	Fuse	8.5 × 4	8
	Line Filter	12 × 8	15
	X-capacitor	12.5 × 5	11
	Choke Coil	Φ8	8
	Film Capacitor	12.5 × 5	11
	PCB	18 × 42	1
	Lead Wire under PCB	-	2
	SMD under PCB	-	1.6
DC Driving Part	Film Capacitor	12.5 × 5	11
	Inductor	18 × 18	14
	Electrolytic Capacitor	Φ12.5 × 20	12.5
	PCB	18 × 45	1
	Lead Wire under PCB	-	2
	SMD under PCB	-	2.4

Table 1 presents the outline information of the main components in each driving part. For the minimized and customized design, small parts were selected to mount them on the G13 enclosure. According to the design calculation, the maximum heights of the AC and DC driving parts are 18 mm and 17.4 mm, respectively, including the PCB thickness and lead wire or SMD parts on the bottom side of the PCB.

III. ELECTRICAL DESIGN

A. CIRCUIT CONFIGURATION AND OPERATION PRINCIPLE

Fig. 7 shows a simplified circuit diagram of the proposed LED converter using a single-stage buck-boost topology, which is operated in discontinuous current mode (DCM). The AC driving part includes a full-bridge rectifier BD and a DC link capacitor C_{DC1}. The DC driving part includes a DC link capacitor C_{DC2}, a switch Q, an inductor L, a diode D, and an output capacitor C_O. An AC voltage with line frequency is applied to the bridge diode through the AC line filter to attenuate the conducted noise or radio frequency. A positive

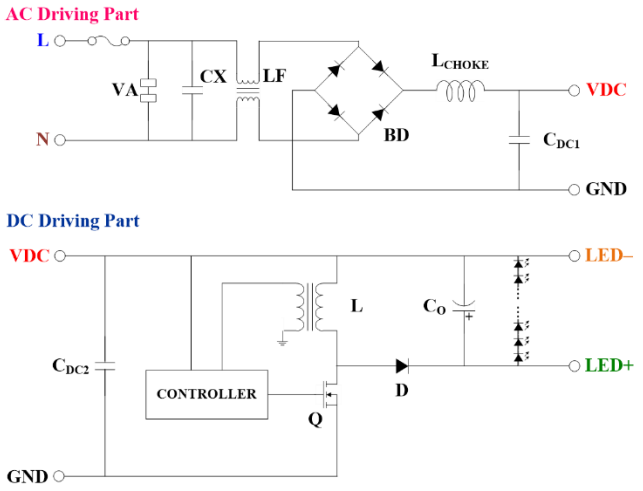

FIGURE 7. Simplified circuit diagram of the proposed LED converter.

full-wave sinusoidal voltage is rectified by a bridge rectifier and transferred to the DC link capacitors C_{DC1} and C_{DC2}.

During the turn-on time of the MOSFET Q, the input energy from the DC link capacitors is stored in the inductor. For the turn-off time, it is transferred to the output capacitor C_O, which is an electrolytic capacitor that is used to supply a current for the LEDs. Since there is a single stage, the output voltage and current have double line frequency ripple. Therefore, a large output capacitance should be chosen to reduce the ripple within the size limit of the converter. The circuit can also be simplified by adopting primary side regulation while removing the photocoupler and secondary feedback control components.

For the PFC operation to obtain high PF and low THD, the switch is controlled when the frequency is too high compared to the line frequency, and the average input current can be made to be sinusoidal and almost the same as the input voltage by using pulse frequency modulation (PFM) [8]–[11]. It is operated at 40-75 kHz in this experiment. Fig. 8 shows the theoretical waveforms of the single-stage buck-boost operated in DCM [12]–[14]. It can be seen that the input current follows the sinusoidal waveform of the input voltage for the basic PFC operation. As a result, a good power factor close unity can be obtained.

B. PARAMETER DESIGN OF THE PROPOSED LED CONVERTER

The rectified input waveform of the single-stage buck-boost in a period and waveform of key components is illustrated in Fig. 8(a)-(b). Some assumptions are made to design the appropriate parameters of the proposed LED converter [2], [9]. First, all the components are ideal, and the parasitic components are ignored. Second, the DC link capacitor is sufficiently small such that V_{DC} is almost the same as the rectified full wave. Third, the switching frequency is much higher than the input line frequency. Therefore, the input voltage is almost constant within a switching cycle. Lastly, half

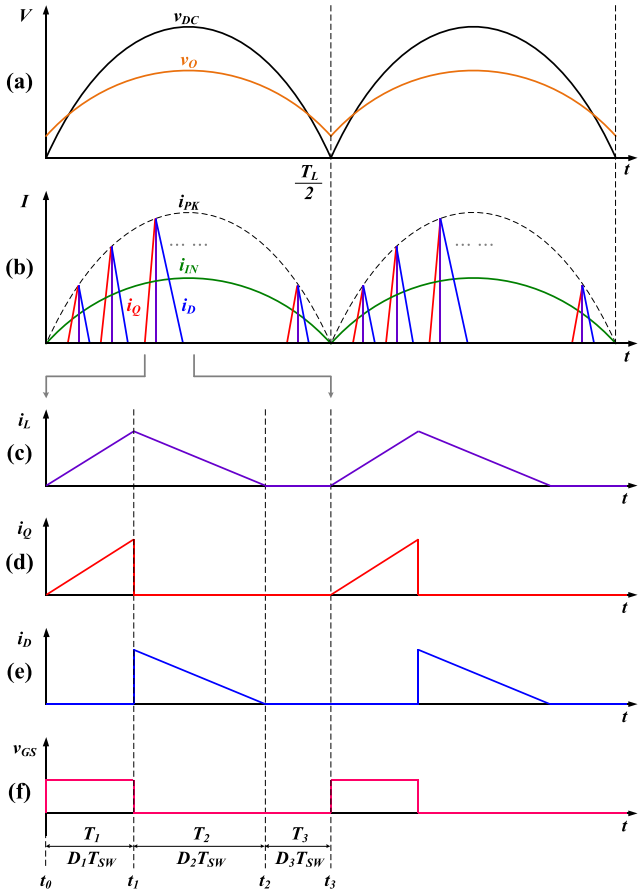

FIGURE 8. Theoretical waveforms of the single-stage buck-boost operated in DCM. (a) rectified input voltage, (b) rectified input current, (c) inductor current, (d) switch current, (e) diode current, and (f) gate-source voltage of switch.

of the line period is only considered ($0 < t < T_L/2$) because of the rectified waveform.

As shown in Fig. 8(a)-(b), the input voltage v_{IN} and input peak current i_{PK} are defined as:

$$v_{IN}(t) = V_{in} \sin(2\pi f_L t) \quad (1)$$

$$i_{PK}(t) = I_{pk} \sin(2\pi f_L t) \quad (2)$$

The single-stage buck-boost LED converter using the PFM method is always operated in DCM. Therefore, the input current i_{IN} is:

$$i_{IN}(t) = \frac{T_1}{2T_{sw}} \cdot I_{pk} \sin(2\pi f_L t) \quad (3)$$

There are three stages during the discontinuous current mode operation in one switching cycle. The first two stages are the switch turn-on and the diode turn-on stage where current flows through the inductor. The remaining stage is the idle state where no more current flows [2], [12]–[15]. Therefore, the time in one switching cycle can be divided into three parts: switch-on time, diode-on time, and idle time,

which are defined as T1, T2, and T3 in Fig. 8(f), respectively:

$$T_{SW} = \frac{T_1}{D_1} = \frac{T_2}{D_2} = \frac{T_3}{D_3} \tag{4}$$

$$T_1 = \frac{L \cdot I_{pk}}{V_{in}} \tag{5}$$

where D_1, D_2, D_3, and L are the duty ratios of each time and the inductance of the inductor, respectively.

From the above equations, equation (6) is derived as:

$$i_{IN}(t) = \frac{L \cdot i_{PK}^2(t) \cdot D_2}{2T_2 \cdot v_{IN}(t)} = \frac{V_o \cdot D_2}{2V_{in}} \cdot I_{pk} sin(2\pi f_L t) \tag{6}$$

$$= \frac{D_1^2 \cdot T_{sw}}{2L} \cdot V_{in} sin(2\pi f_L t) \tag{7}$$

Equations (6) and (7) show that the input current has a sinusoidal shape and has the same phase as the input voltage [2], [12], [13]. Furthermore, from the equations, the key component parameters can be chosen for various in input voltage conditions.

For the next step, the power efficiency should be considered to find the output current. The input power from the AC line is the sum of the power transferred to the LED arrays and the power dissipated in the circuit, $P_{IN} = P_O$ (P_{LED}+ $P_{Dissipation}$), which can be expressed using the power efficiency η_{eff}:

$$P_O = \eta_{eff} \cdot P_{IN} \tag{8}$$

$$V_O \cdot I_O = \eta_{eff} \cdot V_{IN} \cdot I_{IN} \tag{9}$$

$$\frac{V_O^2}{R_O} = \eta_{eff} \cdot \frac{V_{IN}^2}{R_{IN}} \tag{10}$$

where R_{IN} is the equivalent input resistance defined by the division of equations (2) and (7), and R_O is the equivalent output resistance determined by V_O and I_O [2], [13]–[16]. Using equations (1), (7), and (10), the instantaneous value of the output current is calculated as:

$$i_O(t) = \frac{\eta_{eff} \cdot D_2 \cdot I_{pk}}{2} sin^2(2\pi f_L t) \tag{11}$$

$$= \frac{\eta_{eff} \cdot D_2 \cdot I_{pk}}{2} \cdot \frac{1 - \cos(4\pi f_L t)}{2} \tag{12}$$

Equation (12) is derived from equation (11) using the sum and difference formulas for the cosine. As shown in equation (12), the output current and output voltage always have double line frequency ripple [10], [17], [18]. Therefore, it is important that a large output capacitance is applied to reduce the peak-to-peak value of the output voltage while considering the output capacitor size. Finally, the average output current is:

$$I_{O_AVG} = \frac{2}{T_L} \int_0^{\frac{T_L}{2}} i_O(t)\, dt = \frac{\eta_{eff} \cdot D_2 \cdot I_{pk}}{4} \tag{13}$$

Therefore, from equation (13), constant output current can be perfectly obtained with various parameter designs.

DCM operation should be considered to choose the inductance of the main inductor. To ensure DCM operation in the whole range of the input and output conditions, times T1 and T2 should satisfy the following:

$$T_1 + T_2 < T_{SW} \tag{14}$$

Equation (13) can be substituted with the duty ratios D_1 and D_2 as below:

$$D_1 + D_2 < 1 \tag{15}$$

The sum of D_1 and D_2 should always be less than 1 because the idle time T_3 should not be zero.

By the volt-second law,

$$V_{IN} \cdot D_1 + (-V_O) \cdot D_2 = 0 \tag{16}$$

By substituting equation (16) into equation (15), inequality (15) becomes:

$$D_1 < \frac{V_O}{V_O + V_{IN}} \tag{17}$$

Using equations (1), (7), and (10), D_1 can be derived as follows:

$$D_1 = \frac{V_O}{V_{IN}} \cdot \sqrt{\frac{2L}{\eta_{eff} \cdot R_O \cdot T_{sw}}} \tag{18}$$

Therefore, combining equations (17) and (18) and rearranging for L results in:

$$\frac{V_O}{V_{IN}} \cdot \sqrt{\frac{2L}{\eta_{eff} \cdot R_O \cdot T_{sw}}} < \frac{V_O}{V_O + V_{IN}} \tag{19}$$

The inductance at the switching frequency $f_{SW}(1/T_{SW})$ is then obtained as:

$$L < \frac{\eta_{eff} \cdot R_O}{2f_{sw}} \cdot \left(\frac{V_{IN}}{V_O + V_{IN}}\right)^2 \tag{20}$$

Consequently, the inductance can be found to maintain DCM operation from equation (20). The minimum inductance will be determined at V_{O_MAX}, V_{IN_MIN}, and f_{SW_MAX} [12]–[14]. The inductance must be selected carefully as a marginal value since the equation was simplified by ignoring various values such as the diode voltage drop and parasitic resistance.

After finding the inductance value, the allowed output current and voltage ripple should be considered to choose the appropriate output capacitance. To achieve a percent flicker specification less than 30%, the allowable peak-to-peak value of the unit LED current, I_{LED_PP}, should be determined from the luminous intensity and current relation curve on the LED datasheet [19]–[21]. I_{LED_PP} is:

$$I_{LED_PP} = I_{LED_MAX} - I_{LED_MIN} \tag{21}$$

which means that I_{LED_MAX} is the current value at 15% higher luminous intensity, and I_{LED_MIN} is the current value at 15% lower luminous intensity.

$$V_{LED\_PP} = V_{LED\_MAX} - V_{LED\_MIN} \tag{22}$$

$$V_{O\_PP} = N_S \cdot V_{LED\_PP} \tag{23}$$

The peak-to-peak value of the unit LED voltage, V_{LED_PP}, is determined from the V-I characteristics curve. The peak-to-peak value of the output voltage is given by equation (23), where N_S is the number of LEDs in series [19], [24]. The output capacitance can be found as follows:

$$C_O = \frac{I_{O\_PP}}{4\pi f_L \cdot V_{O\_PP}} = \frac{2I_{O\_AVG}}{4\pi f_L \cdot N_S \cdot V_{LED\_PP}} \quad (24)$$

Finally, the output capacitance is determined at the minimum line frequency of 50 Hz. A large capacitance should be used to obtain good flicker performance. However, it should be carefully applied to consider the flicker performance and size since the size of the capacitor increases as the capacitance rises.

IV. EXPERIMENTAL RESULTS

For the experiment, a prototype was designed based on a DCM single-stage buck-boost topology with separation of the AC and DC driving parts for a 19-W T8 LED tube. Table 2 shows the specifications and key component values of the proposed LED converter. The number of LEDs is determined by the requirement of the optical performance. Thus, the output voltage is 196 V when using 66 LEDs in series.

TABLE 2. (a) Specifications of the proposed LED converter, (b) Specifications of key components.

Specification of the proposed LED converter	
Line Voltage	100-240VAC
Line Frequency	50/60Hz
Power Consumption	19W
Output Voltage	196V
Output Current	89mA

(a)

Specification of key components		
AC Driving Part	**Fuse**	250V, 1A
	Line Filter	TOROIDAL, 31uH, 4A
	X-capacitor	275VAC, 100nF
	Bridge Diode	V_{RRM}=1000V, I_O=1A
	Film Capacitor	600V, 100nF
	PCB	CEM-3, 1T, 0.5oz, Single Layer
DC Driving Part	**Film Capacitor**	630V, 100nF
	Inductor	EE1616, 1.38mH
	Electrolytic Capacitor	400V, 22uF, 105℃
	FET	VDSS=800V, I_D=2.5A, $R_{DS(ON)}$<4.5Ω
	Diode	V_{RRM}=1000V, I_O=1A
	PCB	FR-4, 1T, 0.5oz, Double Layer

(b)

The waveform of the input voltage and current in each condition was measured, as shown in Fig. 9. The input

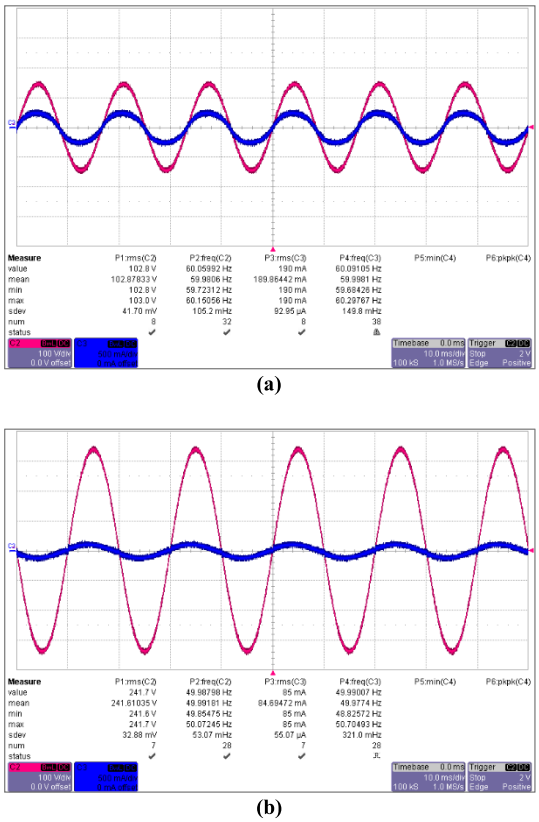

(a)

(b)

FIGURE 9. Waveform of the input voltage (red) and current (blue) (a) at 100 VAC, 60 Hz, (b) 240 VAC, 50 Hz.

current is exactly a sinusoidal waveform that follows the input voltage. The power factor correction operation with constant current control works well. Fig. 10 illustrates the waveform of the output voltage and current. As explained in the prior section, the double line frequency and peak-to-peak values are determined by the output capacitance and LED I-V characteristics. The design was meant to achieve percent flicker less than 30%, and as a result, the peak-to-peak current is about 60 mA.

The measured power efficiency according to the input voltage is shown in Fig. 11. The circuit efficiency is more than 89% throughout the range of 100-240 VAC, and there is almost no difference between 50 Hz and 60 Hz. Particularly, the measured results show that the circuit efficiency is slightly better around the middle of the input voltage range because the regulation of the output current is better than at lower or higher input voltages.

Fig. 12 shows the measured output current from the proposed LED converter to the LED module using 66 LEDs in series. The average measured output current and its standard deviation were 89.3 mA and 1.7 mA, respectively. The positive and negative maximum deviations from the average output current were calculated as +3.1 mA (3.36%) and -2.7 mA (3.02%) at 50 Hz and 60 Hz. This is good performance with primary side regulation since the power consumption tolerance is usually permitted ±10%.

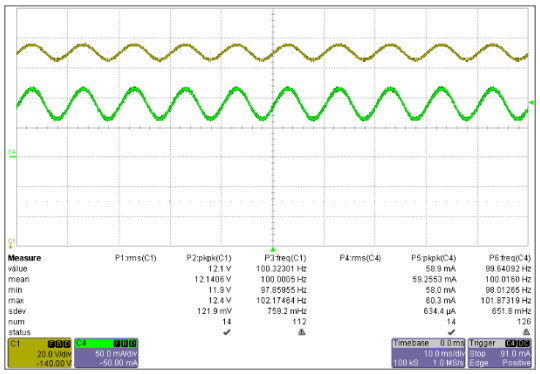

FIGURE 10. Waveform of output voltage (yellow) and current (green) (a) at the 100 VAC, 60 Hz, (b) 240 VAC, 50 Hz.

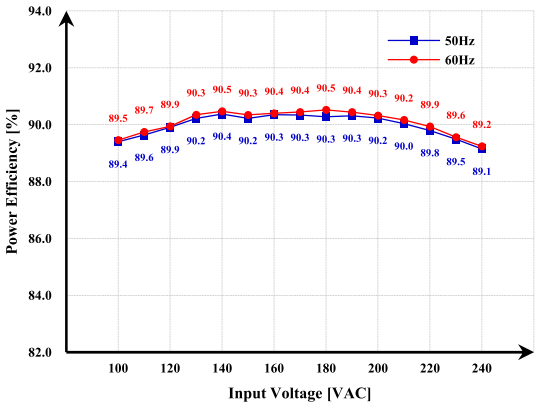

FIGURE 11. Power efficiency according to the input voltage.

The power factor is defined as the ratio of the real power that is used to turn on the LED tube to the apparent power that is provided to circuit:

$$PowerFactor = \frac{RealPower}{ApparentPower}$$

The power factor is dimensionless and ranges from 0 to 1. A power factor close to 1 indicates the voltage and current have almost the same phase. Fig. 13 shows the measured power factor in the range of 100-240 VAC. The measured

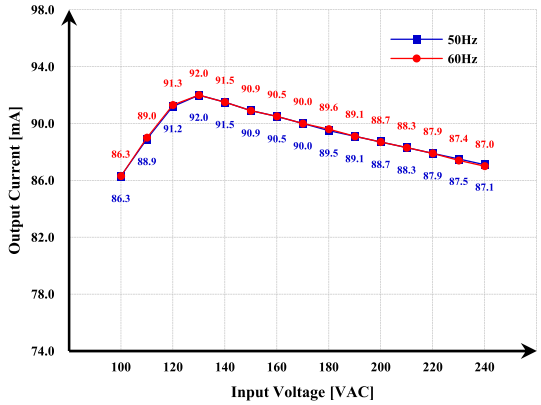

FIGURE 12. Output current according to the input voltage.

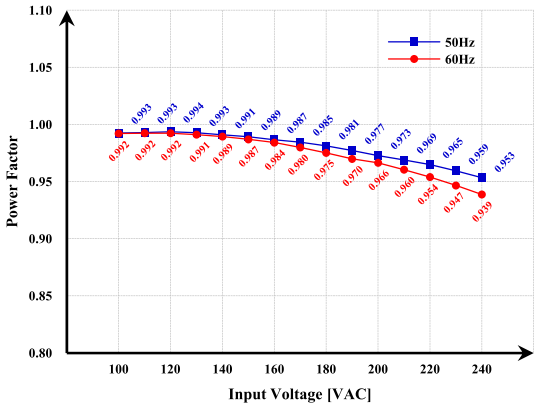

FIGURE 13. Power factor according to the input voltage.

value is higher than 0.93 under all input conditions and slightly decreases as the input voltage increases.

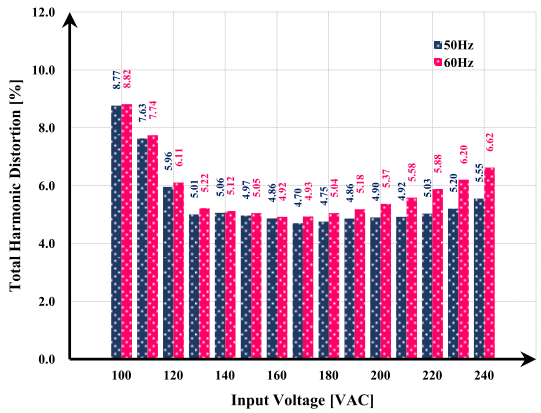

FIGURE 14. Total harmonic distortion according to the input voltage.

Fig. 14 shows the measured total harmonic distortion of the proposed LED converter, which is less than 9% under all input conditions. The values of THD at 100 VAC are 8.77% and 8.82% at 50 Hz and 60 Hz, respectively. At 240 VAC, the values are 5.55% at 50 Hz and 6.62% at 60 Hz, respectively. Therefore, it is suitable for a high-performance LED tube.

Fig. 15 shows the measured results of the harmonic current under various operation conditions. The maximum

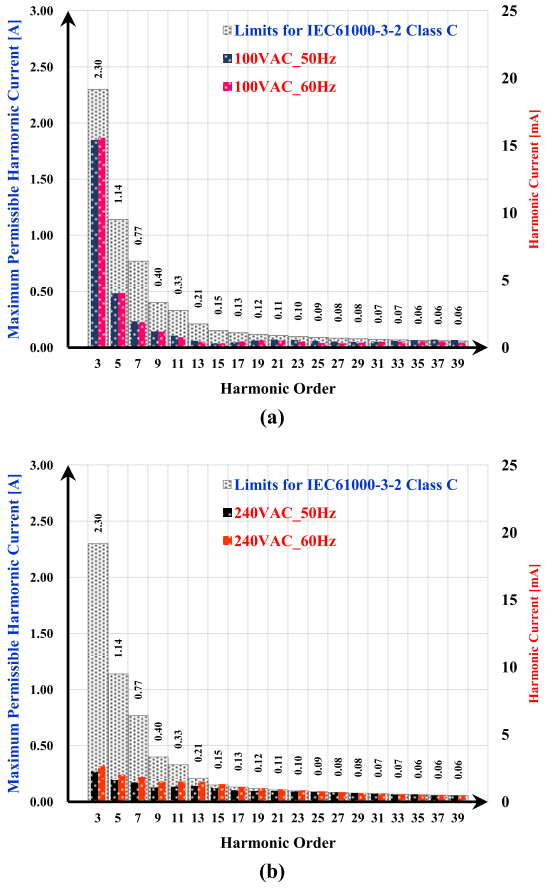

FIGURE 15. Harmonic current according the harmonic order at (a) 100 VAC and (b) 240 VAC.

permissible harmonic current from the IEC 61000-3-2 Class C standard for less than 25 W for lighting is presented with a gray bar [25]. The measured current is significantly lower than the IEC specifications in all conditions.

V. CONCLUSION

In this paper, a new high-performance LED converter has been proposed to solve various problems of a conventional T8 LED tube. The proposed LED converter adopts separation of the AC and DC driving parts for light uniformity and a single-stage buck-boost topology for a wide input rage. A prototype for a 19 W T8 LED tube was successfully manufactured to verify the high performance. The outline of the proposed LED converter was 18 mm × 42mm × 20 mm (W×L×H) for the AC driving part and 18 mm × 45 mm × 20 mm (W×L×H) for the DC driving part, which were optimized to be inserted in a G13 base and G13 base dummy, respectively. The experimental results showed that the line regulation of the LED output current was less than 3.4% at 100-240 VAC and achieved high circuit efficiency (>89%), a high power factor (>0.93), and low total harmonic distortion (<9%). In addition, all the current harmonics of the proposed LED converter met the requirements of the IEC 61000-3-2 Class C standard at input voltages of 100 VAC and 240 VAC for high-performance LED lighting applications.

REFERENCES

[1] D. G. Lamar, M. Arias, M. M. Hernando, and J. Sebastian, "Using the loss-free resistor concept to design a simple AC–DC HB-LED driver for retrofit lamp applications," *IEEE Trans. Ind. Appl.*, vol. 65, no. 3, pp. 2300–2311, May/Jun. 2015.

[2] Y.-C. Chuang, Y. L. Ke, H. S. Chuang, and C. C. Hu, "Single-stage power-factor-correction circuit with flyback converter to drive LEDs for lighting applications," in *Proc. IEEE Ind. Appl. Soc. Annu. Meeting*, Oct. 2010, pp. 1–9.

[3] J. Zhao, Y. Liu, H. Tang, S. Y. Leung, C. C. Yuan, and G. Q. Zhang, "A novel design of heatsink-less LED base fluorescent lamp retrofit," in *Proc. 15th Int. Conf. Electron. Packag. Technol.*, Aug. 2014, pp. 1202–1207.

[4] J. Shao and T. Stamm, "A cost effective high performance LED driver powered by electronic ballasts," in *Proc. IEEE Appl. Power Electron. Conf. Expo. (APEC)*, 2016, pp. 3659–3662.

[5] T. J. Liang, W. J. Tseng, W. R. Chen, and J. F. Chen, "Design and implementation of retrofit LED lamp for fluorescent lamp driven by electronic, electromagnetic ballast and AC mains," in *Proc. IEEE IFEEC*, Nov. 2013, pp. 585–589.

[6] N. Chen and H. S.-H. Chung, "A driving technology for retrofit LED lamp for fluorescent lighting fixtures with electronic ballasts," *IEEE Trans. Power Electron.*, vol. 26, no. 2, pp. 588–601, Feb. 2011.

[7] *Lamp Caps and Holders Together With Gauges for The Control Of Interchangeability and Safety—PART 1: LAMP CAPS*, Standard IEC 60061-1, 2005.

[8] C. Trujillo, G. Henao, J. Castro, and A. Narvaez, "Design and development of a LED driver prototype with a single-stage PFC and low current harmonic distortion," *IEEE Latin Amer. Trans.*, vol. 15, no. 8, pp. 1368–1375, Aug. 2017.

[9] C.-A. Cheng, C.-H. Chang, H.-L. Cheng, and T.-Y. Chung, "A single-stage high-PF driver for supplying a T8-type LED lamp," in *Proc. Int. Power Electron. Conf.*, May 2014, pp. 2523–2528.

[10] Y. Wang, S. Zhang, J. M. Alonso, X. Liu, and D. Xu, "A single-stage LED driver with high-performance primary-side-regulated characteristic," *IEEE Trans. Circuits Syst., II, Exp. Briefs*, vol. 65, no. 1, pp. 76–80, Jan. 2018.

[11] B. White, H. Wang, Y.-F. Liu, and X. Liu, "An average current modulation method for single-stage LED drivers with high power factor and zero low-frequency current ripple," *IEEE J. Emerg. Sel. Topics Power Electron.*, vol. 3, no. 3, pp. 714–731, Sep. 2015.

[12] C. Lei, "Single stage primary side regulation PFC controller for LED driver," Diodes Incorporated, Plano, TX, USA, Tech. Rep., Dec. 2015.

[13] E. Rogers, "Understanding buck-boost power stages in switch mode power supplies," Texas Instruments, Dallas, TX, USA, Tech. Rep., 2007.

[14] H. Fan, "Design tips for an efficient non-inverting, buck-boost converter," Texas Instruments, Dallas, TX, USA, Tech. Rep., 2014.

[15] C. Adragna, "Design equations of high-power-factor flyback converters based on the L6561," STMicroelectronics, Appl. Note AN1059, 2003.

[16] H. Y. Jung, S. H. Kim, B. Moon, and S.-H. Lee, "A new circuit design of two-switch buck-boost converter," *IEEE Access*, vol. 6, pp. 47415–47423, Aug. 2018.

[17] Y. Qiu, L. Wang, H. Wang, Y.-F. Liu, and P. C. Sen, "Bipolar ripple cancellation method to achieve single-stage electrolytic-capacitor-less high-power LED driver," *IEEE J. Emerg. Sel. Topics Power Electron.*, vol. 3, no. 3, pp. 698–713, Sep. 2015.

[18] P. S. Almeida *et al.*, "Static and dynamic photoelectrothermal modeling of LED lamps including low-frequency current ripple effects," *IEEE Trans. Power Electron.*, vol. 30, no. 7, pp. 3841–3851, Jul. 2015.

[19] *SSC-STW8QI4BE Technical Data Sheet*, Seoul Semiconductor, Ansan, South Korea, Sep. 2012.

[20] M. E. Poplawski and N. M. Miller, "Flicker in solid-state lighting: Measurement techniques, and proposed reporting and application criteria," presented at the CIE Centenary Conf., Paris, France, 2013.

[21] *A Review of the Literature on Light Flicker: Ergonomics, Biological Attributes, Potential Health Effects, and Methods in Which Some LED Lighting May Introduce Flicker*, IEEE Standard P1789, Feb. 2010.

[22] R. Van Roy, "Minimizing light flicker in LED lighting applications," Richtek Technol., Appl. Note AN022, Jul. 2014.

[23] C. S. Wong, K. H. Loo, Y. M. Lai, M. H. L. Chow, and C. K. Tse, "An alternative approach to LED driver design based on high-voltage driving," *IEEE Trans. Power Electron.*, vol. 31, no. 3, pp. 2465–2475, Mar. 2016.
[24] S. Wang, X. Ruan, K. Yao, S.-C. Tan, Y. Yang, and Z. Ye, "A flicker-free electrolytic capacitor-less AC–DC LED driver," *IEEE Trans. Power Electron.*, vol. 27, no. 11, pp. 4540–4548, Nov. 2012.
[25] *PFC Harmonic Current Emissions—Guide to EN61000-3-2:2014*, EPSMA Technical Committee, Jul. 2018.

SUNG HWAN KIM received the B.S. degree in electrical engineering, and the M.S. degree in plasma display engineering from Inha University, Incheon, South Korea, in 2003 and 2005, respectively, where he is currently pursuing the Ph.D. degree. His research is currently focused on converters for LED lighting and LED displays.

SEOK-HYUN LEE received the B.S. degree in electrical engineering, and the M.S. and Ph.D. degrees in plasma engineering from Seoul National University, Seoul, South Korea, in 1985, 1987, and 1993, respectively. He was with the Semiconductor Research Center, Hyundai Electronics, Seoul, from 1993 to 1995. Since 1995, he has been a Professor with the Department of Electrical Engineering, Inha University, Incheon, South Korea. His research is currently focused on converter topology design, new renewable energy technology, and power electronics.